

## Supporting Information

**Title** High performance and stable nonfullerene acceptor-based organic solar cells for indoor to outdoor light

Sungmin Park,<sup>†,‡</sup> Hyungju Ahn,<sup>§,‡</sup> Ji-yeong Kim,<sup>†,¶</sup> Jong Baek Park,<sup>†</sup> Junghwan Kim,<sup>†</sup> Sang Hyuk Im,<sup>¶</sup> and Hae Jung Son<sup>\*,†,‡,⊥</sup>

<sup>†</sup>Photo-electronic Hybrids Research Center, Korea Institute of Science and Technology, Seoul 02792, Republic of Korea

<sup>‡</sup>Division of Energy and Environment, KIST School, University of Science and Technology (UST), Daejeon 34113, Republic of Korea

<sup>⊥</sup>KU-KIST Graduate School of Energy and Environment, Seongbuk-Gu, Seoul 02841, Republic of Korea

<sup>§</sup>Pohang Accelerator Laboratory, Kyungbuk, Pohang 37673, Korea

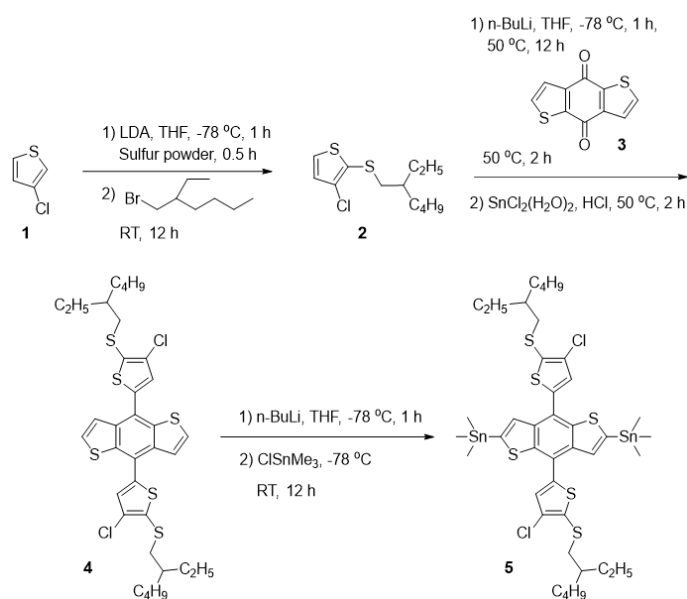
<sup>¶</sup>Department of Chemical and Biological Engineering, Korea University, Seoul 02792, Republic of Korea

### Experimental Section

**General:** Unless stated otherwise, all of chemicals and solvents for synthesis, characterization, and device fabrication were purchased from Sigma-Aldrich and used without further purification process. Benzo[1,2-*b*:4,5-*b'*]dithiophene-4,8-dione (**3**) and 1,3-bis(5-bromothiophen-2-yl)-5,7-bis(2-ethylhexyl)benzo[1,2-*c*:4,5-*c'*]dithiophene-4,8-dione (**6**) were purchased from Sunatech and tetrakis(triphenylphosphine)palladium(0) was purchased from Stream as bright yellow crystal. All of synthesized products were characterized by measuring the <sup>1</sup>H and <sup>13</sup>C NMR using a Bruker Ascend 400 spectrometer in CDCl<sub>3</sub> at 298 K and <sup>1</sup>H NMR of synthesized polymer was obtained in C<sub>2</sub>D<sub>2</sub>Cl<sub>4</sub>. The NMR data were reported by that the chemical shift expressed as parts per million (ppm) on the basis of tetramethylsilane (TMS). For <sup>1</sup>H NMR data, the splitting patterns were shown as singlet (s), doublet (d), doublet of doublet (dd), triplet (t), multiplet (m), and broad (br). The ultraviolet-visible (UV-vis) absorption spectra of the active layer materials were obtained by a PerkinElmer Lambda 35

UV/vis spectrometer. The differential scanning calorimetry (DSC) data of IT-4F and blends were recorded using DSC4000 system of PerkinElmer in the temperature range of 50 °C to 300 °C at the heating rate of 10 °C/min.

### Synthesis of the monomer



**Scheme S1.** Synthetic scheme for the monomer.

**3-chloro-2-((2-ethylhexyl)thio)thiophene (2):** 3-chlorothiophene (**1**) (4.99 g, 42.1 mmol) was added into a completely dried reaction flask and dissolved in anhydrous diethyl ether (84.2 mL). Lithium diisopropylamide (LDA, 1.0 M, 44.2 mL, 44.2 mmol) was added dropwise into the reaction flask at -78 °C and the reaction was kept stir for 1 h at the same temperature. Sulfur powder (1.48 g, 46.3 mmol) was put into the reaction flask and the reaction was performed for

additional 30 min. And then, 2-ethylhexyl bromide (9.75 g, 50.5 mmol) was injected into the reaction and the reaction was allowed to reach room temperature. After overnight reaction in room temperature, the reaction was quenched with injection of deionized water and then an organic layer was extracted with diethyl ether, dehydrated with MgSO<sub>4</sub> and concentrated by rotary evaporator. Silica gel column chromatography was performed with hexane as eluent to obtain the product. (8.09 g, 73.1%)

<sup>1</sup>H NMR (CDCl<sub>3</sub>, 400 MHz)  $\delta$  (ppm): 7.27 (d, 1H), 6.94 (d, 1H), 2.82 (d, 2H), 1.15-1.53 (m, 9H), 0.81-0.93 (m, 6H). <sup>13</sup>C NMR (CDCl<sub>3</sub>, 100 MHz)  $\delta$  (ppm): 130.10, 129.51, 128.23, 127.10, 42.05, 39.06, 32.09, 28.75, 25.34, 22.96, 14.11, 10.73.

**4,8-bis(4-chloro-5-((2-ethylhexyl)thio)thiophen-2-yl)benzo[1,2-*b*:4,5-*b'*]dithiophene (4):** 3-chloro-2-((2-ethylhexyl)thio)thiophene (**2**)(4.03 g, 15.3 mmol) was added into a completely dried reaction flask and dissolved in anhydrous tetrahydrofuran (THF, 30.9 mL). *n*-Butyllithium (*n*-BuLi, 1.6 M, 44.2 mL, 44.2 mmol) was added dropwise into the reaction flask at -78 °C and the reaction was kept stir for 1 h at the same temperature. The reaction flask was warmed up to 50 °C and kept stir overnight. Benzo[1,2-*b*:4,5-*b'*]dithiophene-4,8-dione (**3**)(1.13 g, 5.1 mmol) was put into the flask and the reaction kept stir for 2 h then cooled down to room temperature. Tin(II) chloride dehydrate (SnCl<sub>2</sub>·(H<sub>2</sub>O)<sub>2</sub>, 9.29 g, 41.2 mmol) was dissolved in 20 mL of HCl and the solution was transferred into the reaction flask. After additional 2 h reaction at room temperature, crude was diluted in deionized water and then an organic layer was extracted with ethyl acetate, dehydrated with MgSO<sub>4</sub> and concentrated by rotary evaporator. Silica gel column chromatography was performed with hexane as eluent to obtain the product. (1.68 g, 46.2%)

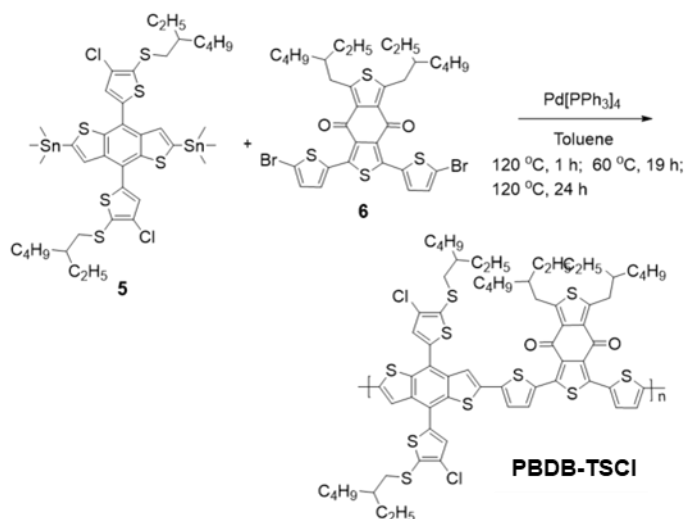
<sup>1</sup>H NMR (CDCl<sub>3</sub>)  $\delta$  (ppm) : 7.59 (d, 2H), 7.52 (d, 2H), 7.31 (s, 2H), 2.96 (dd, 4H), 1.62 (m,

2H), 1.20-1.53 (m, 16H), 0.86-0.97 (m, 12H).  $^{13}\text{C}$  NMR ( $\text{CDCl}_3$ , 100 MHz)  $\delta$  (ppm): 140.33, 139.00, 136.48, 131.07, 129.75, 128.75, 128.43, 122.99, 122.77, 42.08, 39.32, 32.19, 28.84, 25.44, 22.95, 14.14, 10.84.

**(4,8-bis(4-chloro-5-((2-ethylhexyl)thio)thiophen-2-yl)benzo[1,2-*b*:4,5-*b'*]dithiophene-2,6-diyl)bis(trimethylstannane) (5):** 4,8-bis(4-chloro-5-((2-ethylhexyl)thio)thiophen-2-yl)benzo[1,2-*b*:4,5-*b'*]dithiophene (**4**) (1.68 g, 2.4 mmol) was added into a completely dried reaction flask and dissolved in anhydrous tetrahydrofuran (THF, 23.6 mL). *n*-Butyllithium (*n*-BuLi, 1.6 M, 3.2 mL, 5.2 mmol) was added dropwise into the reaction flask at  $-78\text{ }^\circ\text{C}$  and the reaction was kept stirred for 1 h at the same temperature. Trimethyltin chloride solution ( $\text{ClSnMe}_3$ , 1 M, 6.3 mL, 6.3 mmol) was injected into the reaction flask and the reaction was allowed to reach room temperature. After overnight reaction in room temperature, the reaction was quenched with injection of deionized water and then an organic layer was extracted with diethyl ether, dehydrated with  $\text{MgSO}_4$  and concentrated by rotary evaporator. The product was obtained by recrystallization in isopropyl alcohol. (1.57 g, 64.3%)

$^1\text{H}$  NMR ( $\text{CDCl}_3$ )  $\delta$  (ppm) : 7.60 (s, 2H), 7.32 (s, 2H), 2.96 (dd, 4H), 1.64 (m, 2H), 1.23-1.53 (m, 16H), 0.84-0.98 (m, 12H), 0.42 (s, 18H).  $^{13}\text{C}$  NMR ( $\text{CDCl}_3$ , 100 MHz)  $\delta$  (ppm): 143.91, 143.32, 141.25, 137.28, 130.47, 130.24, 129.74, 128.53, 121.23, 42.05, 39.30, 32.15, 28.79, 25.42, 22.93, 14.13, 10.86, -8.26.

## Synthesis of PBDB-TSCI



**Scheme S2.** Synthetic scheme for PBDB-TSCI.

**PBDB-TSCI:** (4,8-bis(4-chloro-5-((2-ethylhexyl)thio)thiophen-2-yl)benzo[1,2-*b*:4,5-*b'*]dithiophene-2,6-diyl)bis(trimethylstannane) (**5**)(311.3 mg, 0.3 mmol), 1,3-Bis(5-bromothiophen-2-yl)-5,7-bis(2-ethylhexyl)benzo[1,2-*c*:4,5-*c'*]dithiophene-4,8-dione (**6**)(230.0 mg, 0.3 mmol) and tetrakis(triphenylphosphine)palladium(0)(7.0 mg, 6.0  $\mu$ mol) were put into a completely dried reaction flask and dissolved in degassed toluene (12 mL). After purge with Ar gas for 20 min, stepwise polycondensation was performed with followed conditions of 120 °C (1 h), 60 °C (19 h), and 120 °C (24 h). Crude polymer was diluted in chlorobenzene and transferred into acetone to precipitate then filtered on thimble filter. Soxhlet extraction was sequentially performed with methanol, hexane, dichloromethane, and chloroform. And then, chloroform fraction was concentrated by rotary evaporator, precipitated in acetone, and filtered to obtained the polymer. (357 mg, 90.4%)

GPC:  $M_n = 20.0$  kg/mol, PDI = 2.38.  $^1\text{H NMR}$  ( $\text{C}_2\text{D}_2\text{Cl}_4$ )  $\delta$  (ppm): 8.35-6.60 (br, 8H), 3.40-2.50 (br, 8H), 2.50-0.20 (br, 56H).

**PBDB-TF:** This polymer was prepared from the modified procedure in the literature.<sup>1,2</sup>

GPC:  $M_n = 14.8$  kg/mol, PDI = 2.28.  $^1\text{H NMR}$  ( $\text{C}_2\text{D}_2\text{Cl}_4$ )  $\delta$  (ppm): 7.95-6.80 (br, 8H), 3.40-2.50 (br, 8H), 2.40-0.20 (br, 60H)

### **Electrochemical properties:**

The cyclic voltammetry (CV) was performed to obtain the highest occupied molecular orbital (HOMO) energy level of polymers using a CH instruments electrochemical analyzer. For all of measurements, 0.1 M tetrabutylammonium hexafluorophosphate ( $\text{Bu}_4\text{NPF}_6$ ) in degassed acetonitrile was used as an electrolyte. Glassy carbon was used as a working electrode, Ag/AgCl as a reference electrode, and Pt wire as a counter electrode in the three electrode system. After polymer samples were loaded on the surface of glassy carbon, CV measurements were conducted with a  $50 \text{ mV s}^{-1}$  potential sweep rate. The HOMO energy levels of PBDB-TF and PBDB-TSCI were estimated by following equation:

$$\text{HOMO (V)} = - [E_{\text{ox}} - E_{1/2}(\text{Fc}/\text{Fc}^+) + 4.8]$$

where  $E_{\text{ox}}$  is the onset oxidation potential of the polymer and  $E_{1/2}(\text{Fc}/\text{Fc}^+)$  is the redox potential of ferrocene/ferrocenium vs. Ag/AgCl.

### **Preparation of polymer solar cell device:**

Polymer solar cells were fabricated with a structure of glass/indium tin oxide (ITO)/ZnO/polymer:IT-4F/ $\text{MoO}_3$ /Ag. Glass substrates with patterned ITO were cleaned by ultrasonication in the order of isopropanol (IPA), acetone, and IPA for 10 min each and dried under  $90^\circ\text{C}$  for 1 hour. After performing the cleaned substrate with an UV/ $\text{O}_3$  cleaner for 20 min, and then the ZnO precursor solution which had been prepared with zinc acetate dehydrate

( $\text{Zn}(\text{CH}_3\text{COO})_2 \cdot 2\text{H}_2\text{O}$ , 1 g) and ethanolamine ( $\text{NH}_2\text{CH}_2\text{CH}_2\text{OH}$ , 0.28 g) dissolved in 2-methoxyethanol ( $\text{CH}_3\text{OCH}_2\text{CH}_2\text{OH}$ , 10 mL) was spin-coated at 5000 rpm and annealed at 200 °C in air. Active layer blend (PBDB-TF:IT-4F/PBDB-TSCI:IT-4F) with ratio of 1:0.8/1:1.2 were dissolved in a mixed solution of chlorobenzene and 1% of 1,8-diiodooctane (DIO) with a concentration of 10/8 mg/ml (for polymer) and stirred for 5 hours at room temperature. The active layer material was spin-coated at 2500/2200rpm on the surface of as-prepared ITO/ZnO substrate then the active layer was treated by thermal annealing at 130 °C for 10 min. A thin layer of  $\text{MoO}_x$  (3 nm), followed by Ag (100 nm) was thermally evaporated through a shadow mask. Active area is 0.044 cm<sup>2</sup>.

Polymer solar cell modules were fabricated with the same structure of single devices and composed of 10-stripe cells connected through a recombination junction of ITO/ZnO/ $\text{MoO}_x$ /Ag.<sup>3</sup> All conditions for cleaning of a stripe-patterned ITO substrate and preparation of the blend solutions and all films are same with the single device. A ZnO and active layers were coated on ITO substrate in sequence and then a thin layer of  $\text{MoO}_x$  (3 nm), followed by Ag (100 nm) was thermally deposited through a shadow mask. The total active area of the module is 58.5 cm<sup>2</sup>.

### **Characterization of polymer solar cell device:**

The photovoltaic performance was measured under AM1.5G at sun light intensity (100 mW/cm<sup>2</sup>) in ambient air with a Keithley model 2400 source meter. The intensity of light was calibrated with a NREL-calibrated Si solar cell coupled with KG-5 filter. Illuminance(lux) of fluorescent lamp was calibrated using a Tenmars TM-208 light lux- and solar power-meter. These calibration data were fitted with points which is obtained from the average of lux and power over 3 min for each illuminance under no other light source. External quantum efficiency

(EQE) was investigated as a function of wavelength on EQE equipment of Mcscience. A NIST-calibrated Si photodiode G425 was used as a standard for calibration.

### **Charge carrier mobility measurements:**

To calculate hole and electron mobility, space-charge-limited current (SCLC) was performed with a Keithley model 2400 source measuring unit in the dark condition. To obtain hole mobility, the diode was fabricated with a structure of ITO/PEDOT:PSS/active layer/Au. For electron-only device, the diode with a structure of ITO/Al/active layer/Al was prepared. The  $J$ - $V$  characteristics of the single carrier devices were calculated from Mott-Gurney law as in following equation,

$$J = \frac{9}{8} \epsilon_r \epsilon_0 \mu \frac{V^2}{L^3}$$

Where  $\epsilon_r$  is the relative permittivity of the material on active layer,  $\epsilon_0$  is the absolute permittivity,  $\mu$  is the charge carrier mobility,  $L$  is the thickness of active film, and  $V$  is the effective voltage calculated by  $V_{\text{appl}} - V_r - V_{\text{bi}}$ , where  $V_{\text{appl}}$  is the applied voltage to the diode,  $V_r$  is the voltage drop across contact resistance and series resistance through the electrodes, and  $V_{\text{bi}}$  is the built-in potential gap induced by the work function difference of two electrodes.<sup>4,5</sup>

### **GIWAXS measurements:**

GIWAXD measurements were conducted at the 9A U-SAXS beamline of the Pohang Light Source (PLS) in South Korea. GIWAXD samples were prepared by spin-coating on <100> silicon wafer with the same fabricating procedures of active layer in optimized device. The wavelength of X-rays was 1.12370 Å ( $E = 11.035$  keV) and the incidence angle of the beam

light was  $0.12^\circ$ . The images from GIWAXD were indicated with a 2D FT-CCD modules of Rayonix MX170-HS. The sample-to-detector distance (SDD) was adjusted to be 224mm.

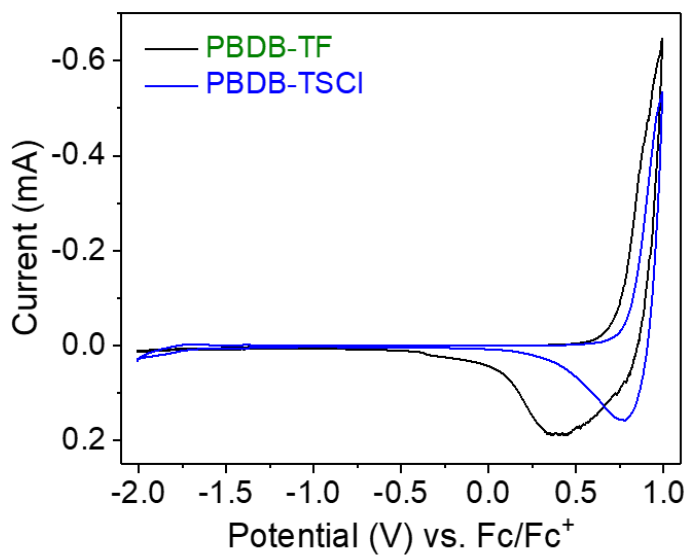


**Figure S1.** Cyclic voltammogram of the polymers.

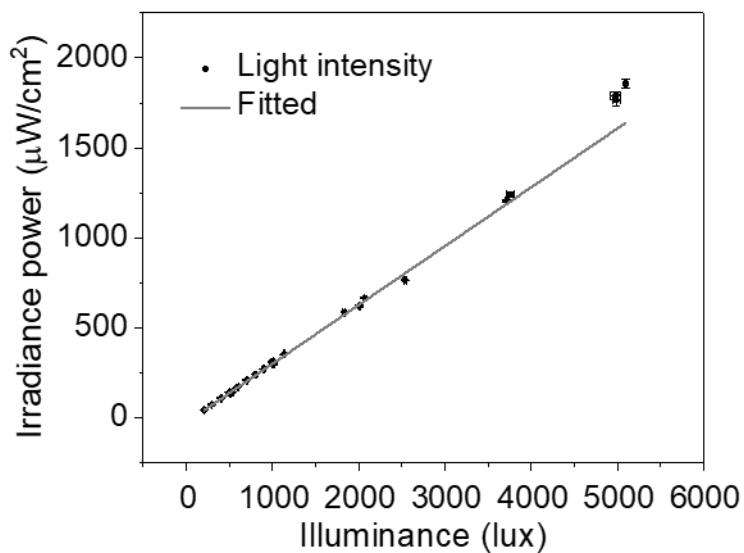


**Figure S2.** Irradiance power-illuminance ratio of fluorescent lamp under no other light source.

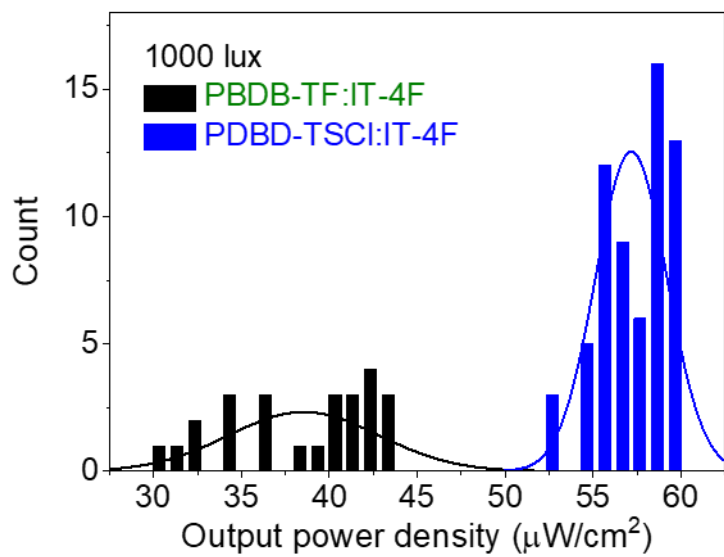


**Figure S3.** Histograms of output power of PBDB-TF and PBDB-TSCI device under 1000 lux illumination.

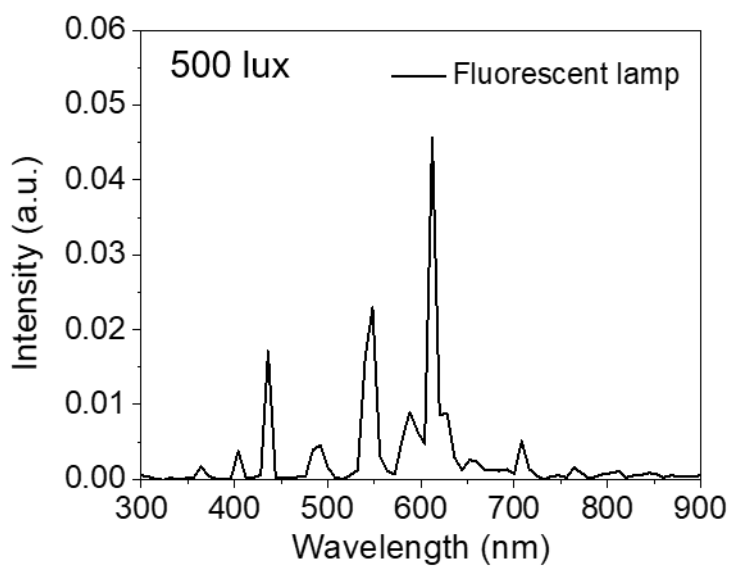


**Figure S4.** Spectrum of the fluorescent lamp

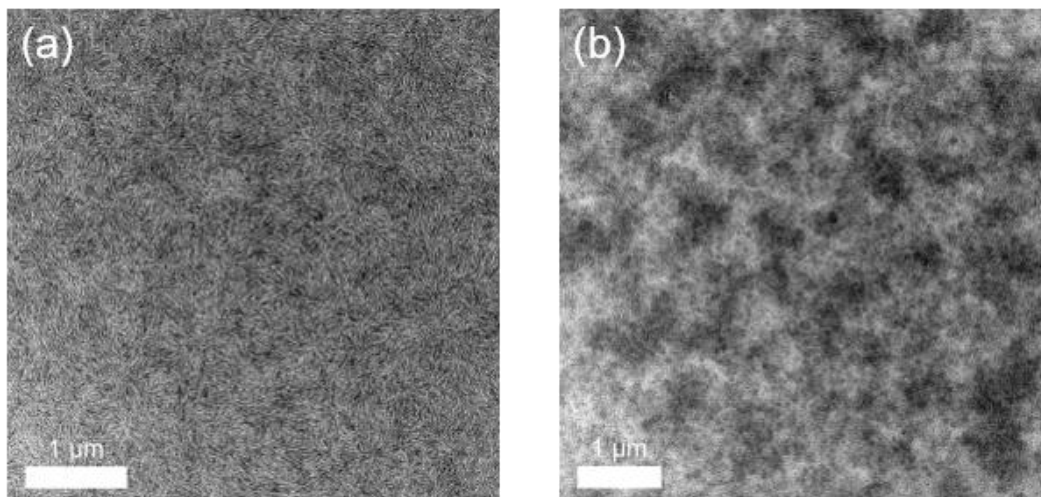


**Figure S5.** TEM images of (a) PBDB-TF and (b) PBDB-TSCI blend film.

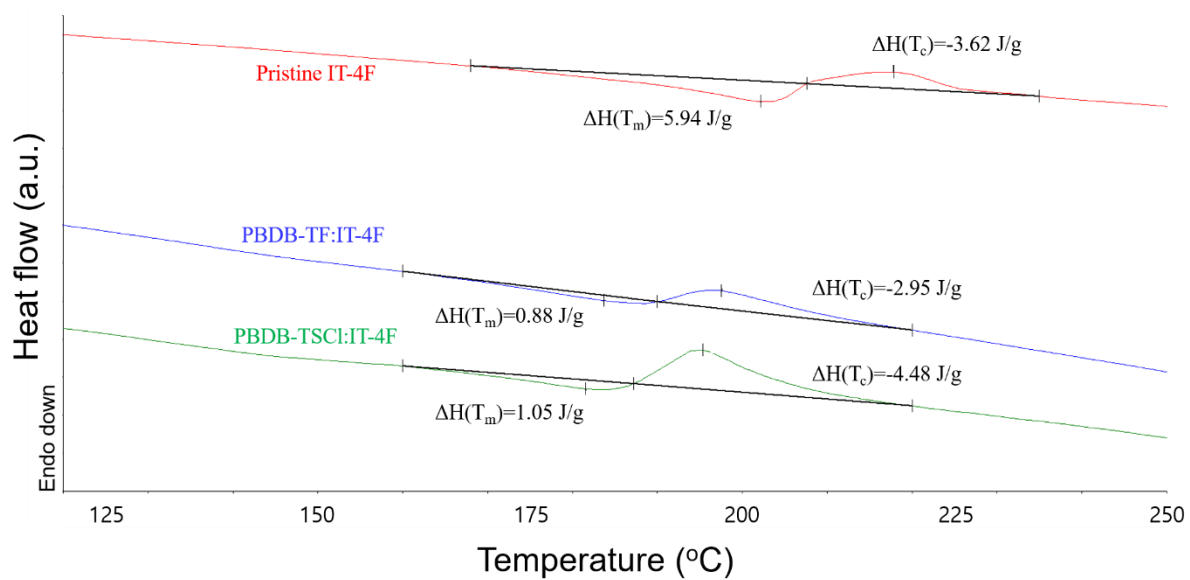


**Figure S6.** First heating DSC thermograms of pristine IT-4F, PBDB-TF:IT-4F, and PBDB-TSCI blend.

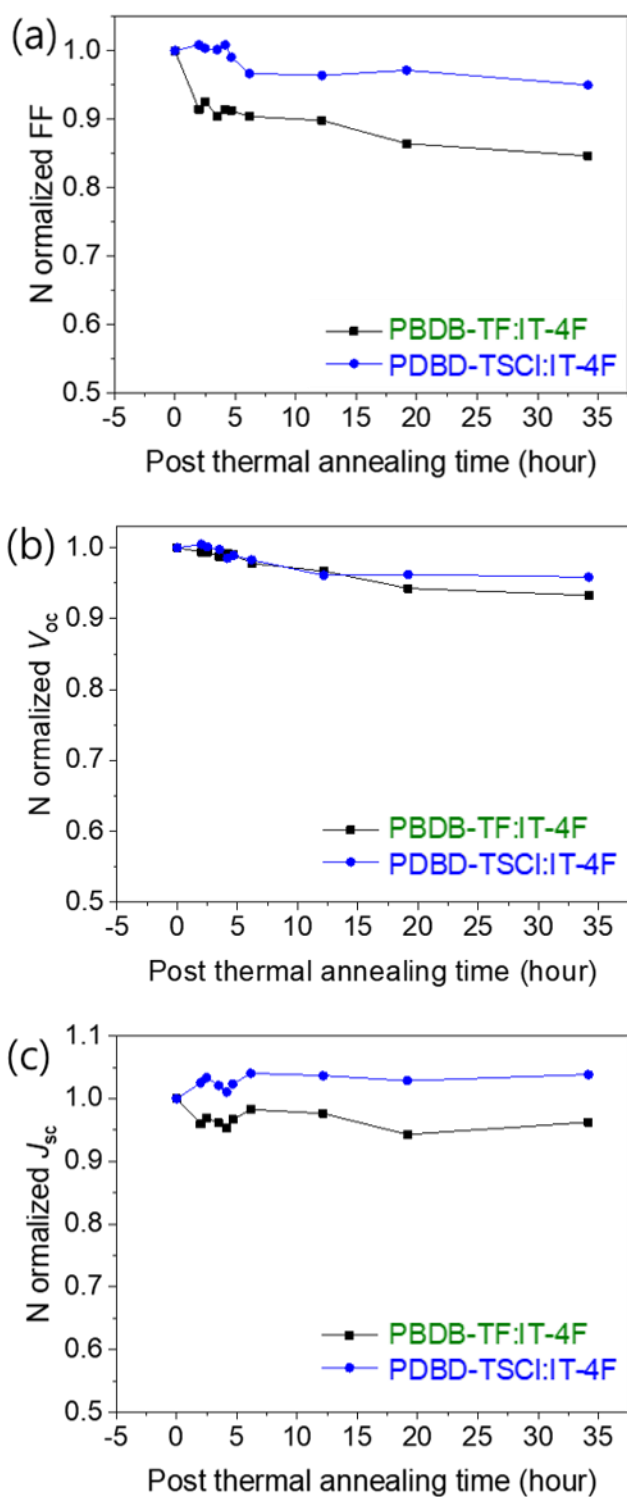


**Figure S7.** Normalized (a) FF, (b)  $V_{oc}$ , and (c)  $J_{sc}$  as a function of time for solar cells of PBDB-TF and PBDB-TSCI aged at 100 °C for 34 hours under an inert atmosphere.

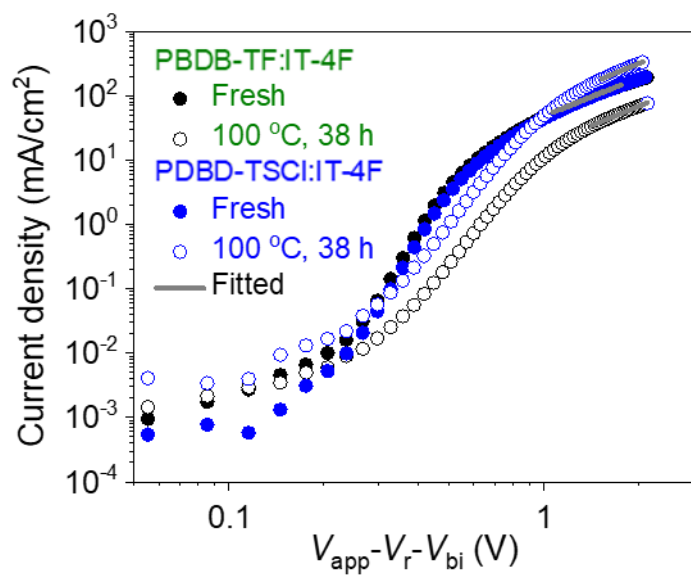


**Figure S8.** Current density-voltage characteristics of hole only device in fresh and after aged at 100 °C for 38 hours under an inert atmosphere.

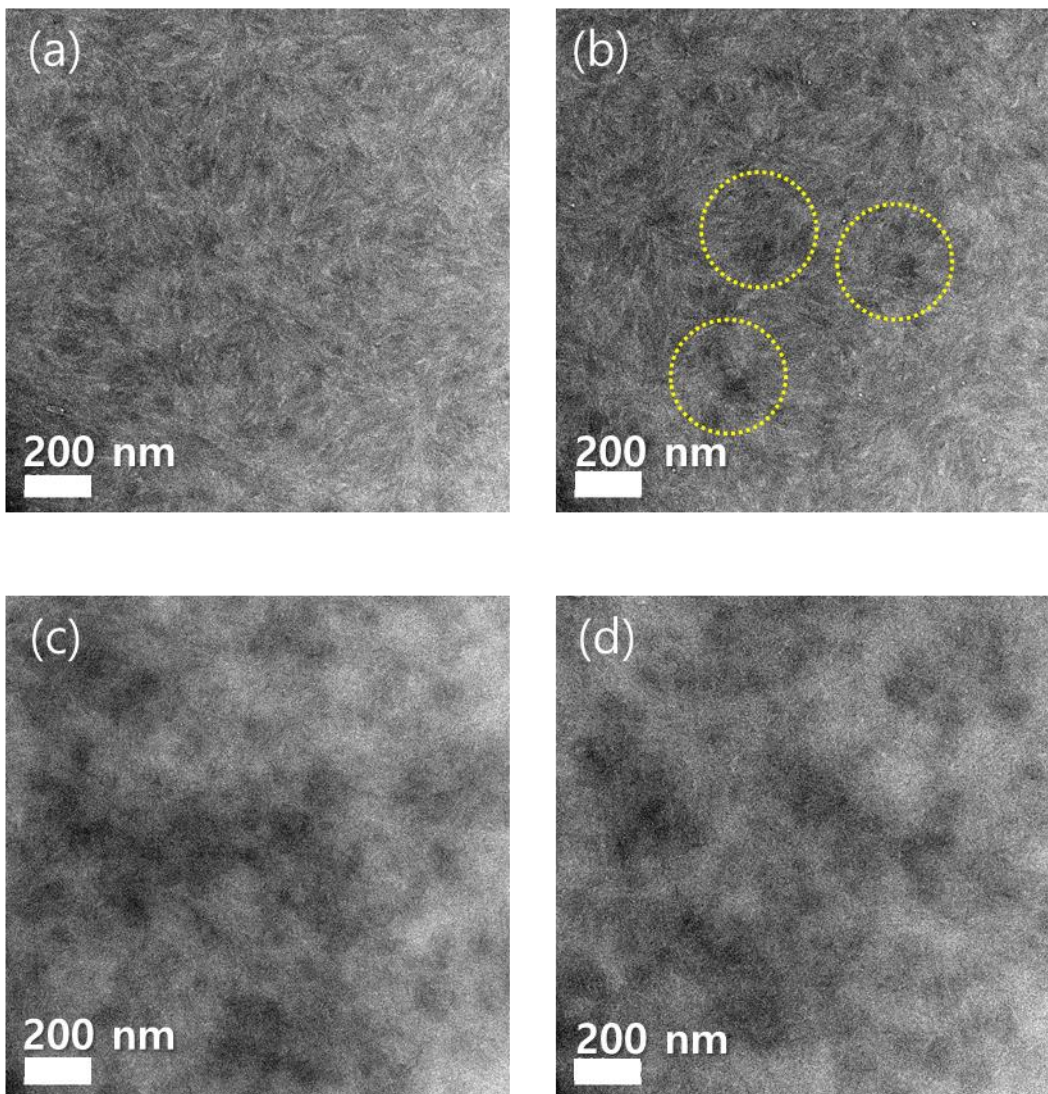


**Figure S9.** TEM images of PBDB-TF(a, b) and PBDB-TSCI (c, d) before (a, c) and after (b, d) aged at 100 °C for 34 hours under an inert atmosphere.

**Table S1.** PCE data of solar cells reported for indoor light.<sup>a</sup>

Light source	Illuminance (intensity)	Active layer	PCE (FF) [%]	Reference
Fluorescent	1000 lux (270 $\mu\text{W}/\text{cm}^2$ )	P3HT:PC <sub>61</sub> BM	7 (74)	Sol. Energy Mater. Sol. Cells 2011, 95, 3256.
	300 lux (83.6 $\mu\text{W}/\text{cm}^2$ )	PCDTBT:PC <sub>71</sub> BM	16.6 (69.3)	Appl. Phys. Lett. 2016, 108, 253301.
	500 lux (164 $\mu\text{W}/\text{cm}^2$ )	P3HT:ICBA	13.76 (62)	Sol. RRL 2017, 1, 1700174.
	300 lux (74 $\mu\text{W}/\text{cm}^2$ )	PCDTBT:PDTSTPD :PC <sub>71</sub> BM	20.8 (63.5)	J. Mater. Chem. A 2018, 6, 8579.
LED	890 lux (364 $\mu\text{W}/\text{cm}^2$ )	PCE10:PC <sub>71</sub> BM	11.63 (74)	Jpn. J. Appl. Phys. 2015, 54, 071602.
	300 lux (77.6 $\mu\text{W}/\text{cm}^2$ )	P1:PC <sub>71</sub> BM	19.15 (66.1)	J. Mater. Chem. C, 2018, 6, 9111.
	500 lux (170 $\mu\text{W}/\text{cm}^2$ )	PTB7:PC <sub>71</sub> BM :EP-PDI	15.68 (68.5)	Chem. Eur. J. 2019, 25, 6154.
	1000 lux (280 $\mu\text{W}/\text{cm}^2$ )	PPDT2FBT :PC <sub>71</sub> BM	16.0 (65.2)	Nano Energy 2019, 58, 466.

<sup>a</sup> The lists of literature which contained input power of indoor light sources and calibration method.

**Table S2.** Calculated dipole moments for the oligomers of PBDB-TF and PBDB-TSCI.

		$\mu_x$ (D)	$\mu_y$ (D)	$\mu_z$ (D)	$\Delta\mu_{ge}$ (D)
PBDB-TF	ground	-0.47	0.31	-0.85	4.12
	excited	-4.52	1.10	-0.74	
PBDB-TSCI	ground	6.10	-0.06	0.93	13.15
	excited	-7.04	0.32	0.84	

$\Delta\mu_{ge}$  = difference between the ground- and excited-state dipole moments

**Table S3.** Comparison of solar cell properties of the PBDB-TF:IT-4F inverted devices prepared using different blend ratios and annealing conditions.

BHJ	Blend ratio	Thermal annealing (TA)	$V_{oc}$ [V]	$J_{sc}$ [mA/cm <sup>2</sup> ]	FF [%]	PCE [%]
PBDB-TF :IT-4F	1:0.8	As cast	0.807	20.40	62.87	10.35
		TA 100 °C, 10 min	0.810	20.37	69.57	11.48
		TA 130 °C, 10 min	0.811	20.85	71.70	12.12
	1:1	As cast	0.792	20.02	68.67	10.89
		TA 100 °C, 10 min	0.789	19.88	67.90	10.65
	1:1.2	As cast	0.788	20.29	66.76	10.67
		TA 100 °C, 10 min	0.782	20.23	68.97	10.91

**Table S4.** Comparison of solar cell properties of the PBDB-TSCl:IT-4F inverted devices prepared using different blend ratios and annealing conditions.

BHJ	Blend ratio	Thermal annealing (TA)	$V_{oc}$ [V]	$J_{sc}$ [mA/cm <sup>2</sup> ]	FF [%]	PCE [%]
PBDB-TSCl :IT-4F	1:0.8	As cast	0.832	20.71	55.9	9.63
		TA 100 °C, 10 min	0.805	21.32	64.68	11.10
	1:1	As cast	0.829	21.1	59.7	10.44
		TA 100 °C, 10 min	0.82	21.28	65.72	11.47
	1:1.2	As cast	0.816	21.46	63.36	11.10
		TA 100 °C, 10 min	0.822	21.29	69.71	12.20
		TA 130 °C, 10 min	0.834	21.17	74.37	13.13

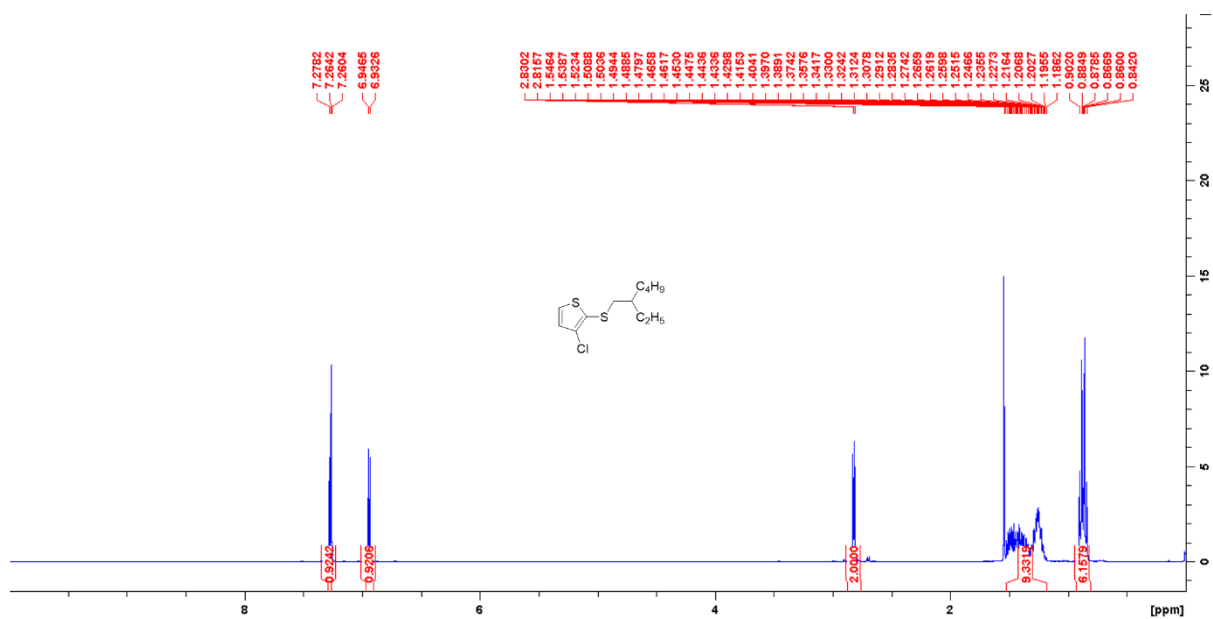


Figure S10. <sup>1</sup>H-NMR spectrum of compound 2

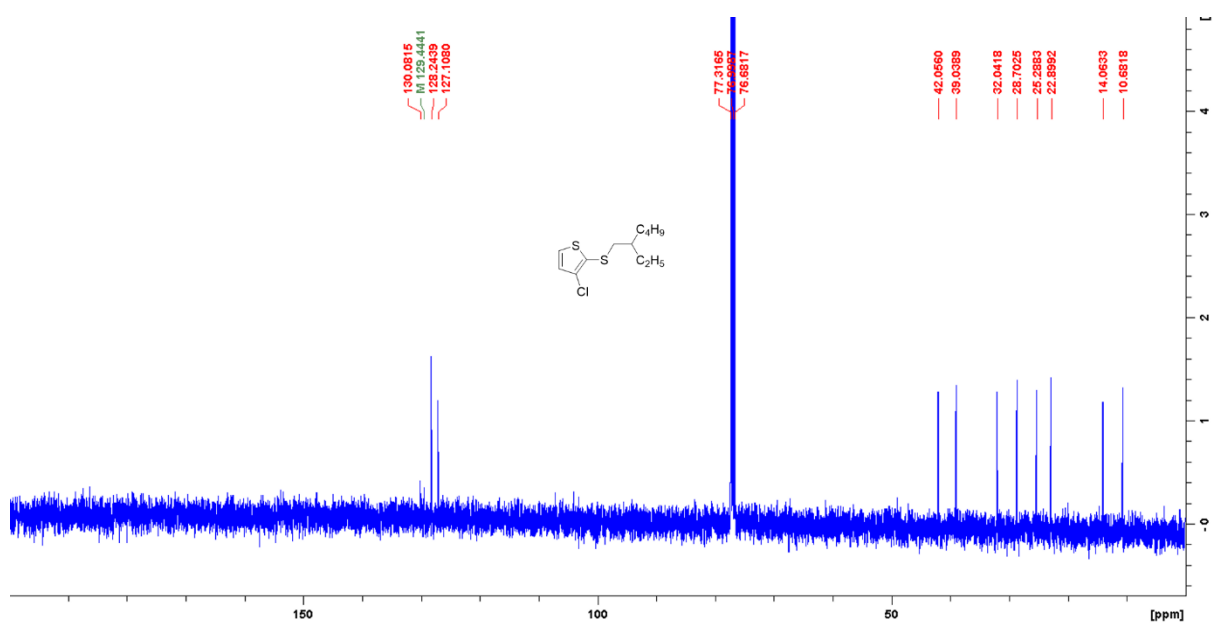


Figure S11. <sup>13</sup>C-NMR spectrum of compound 2

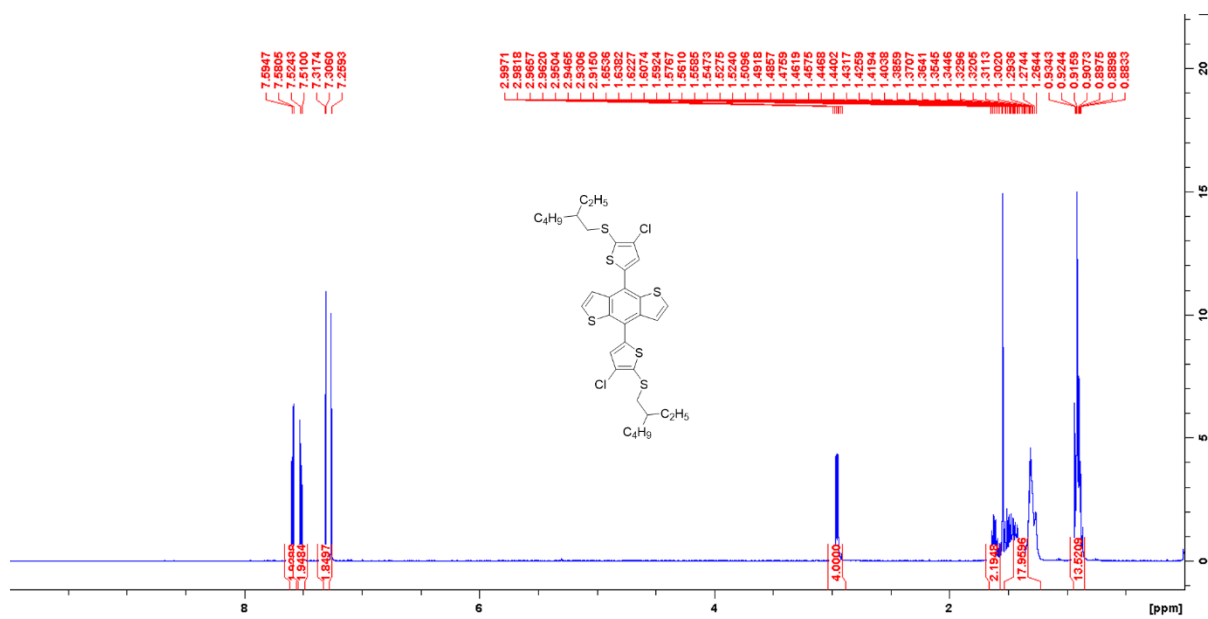


Figure S12. <sup>1</sup>H-NMR spectrum of compound 4

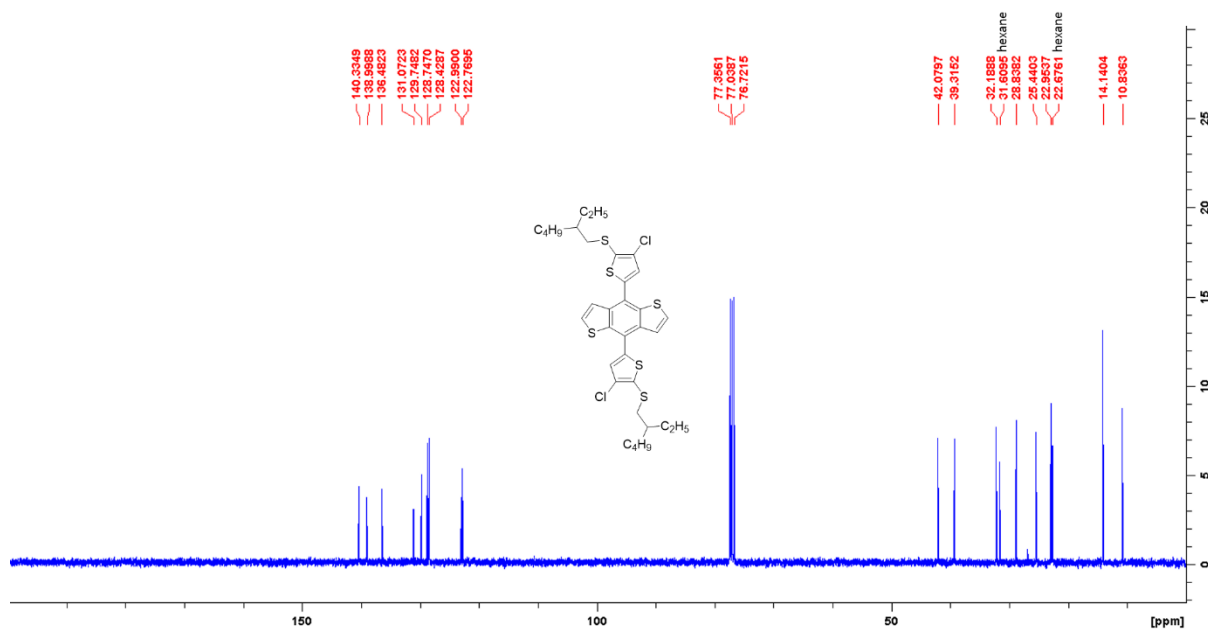


Figure S13. <sup>13</sup>C-NMR spectrum of compound 4

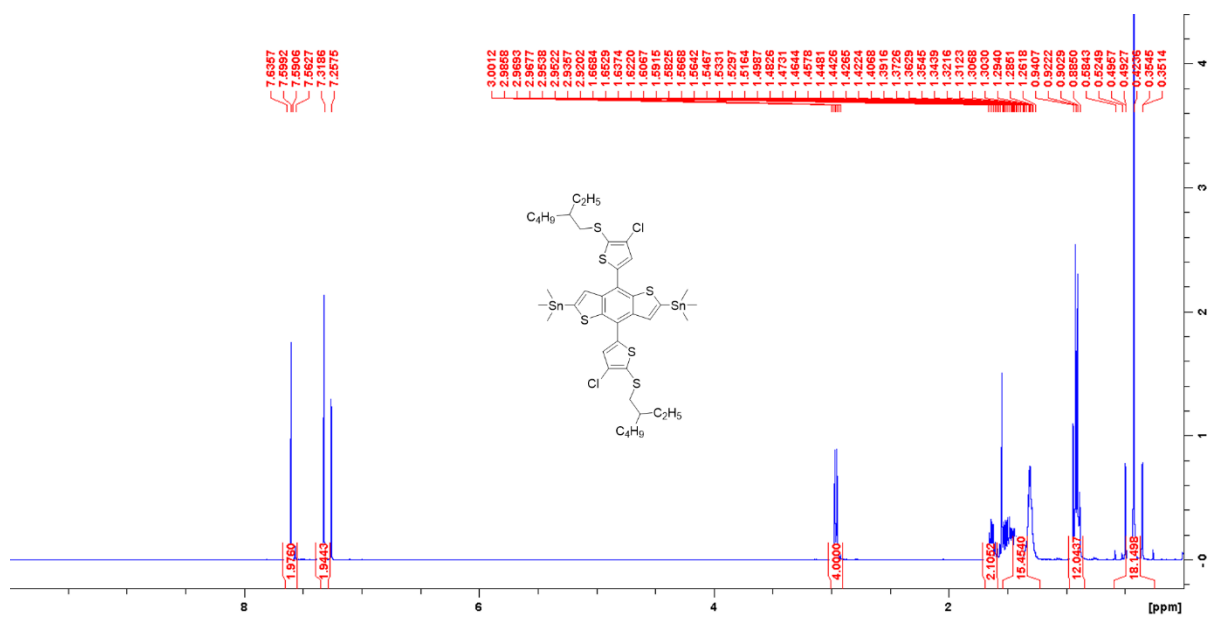


Figure S14. <sup>1</sup>H-NMR spectrum of compound 5

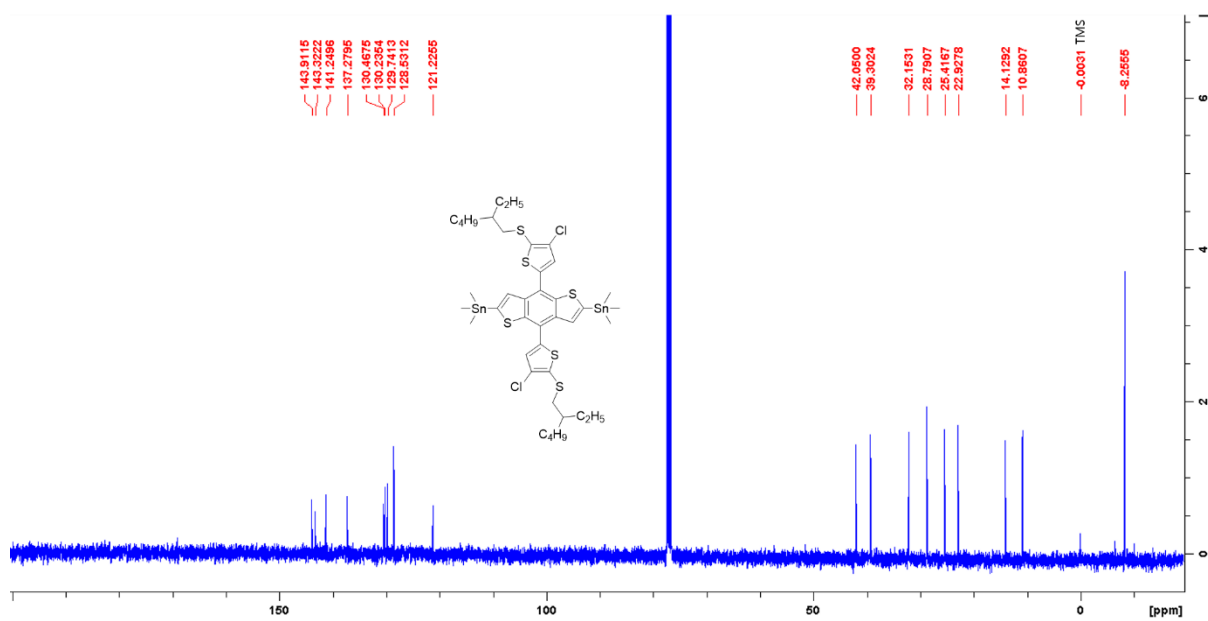
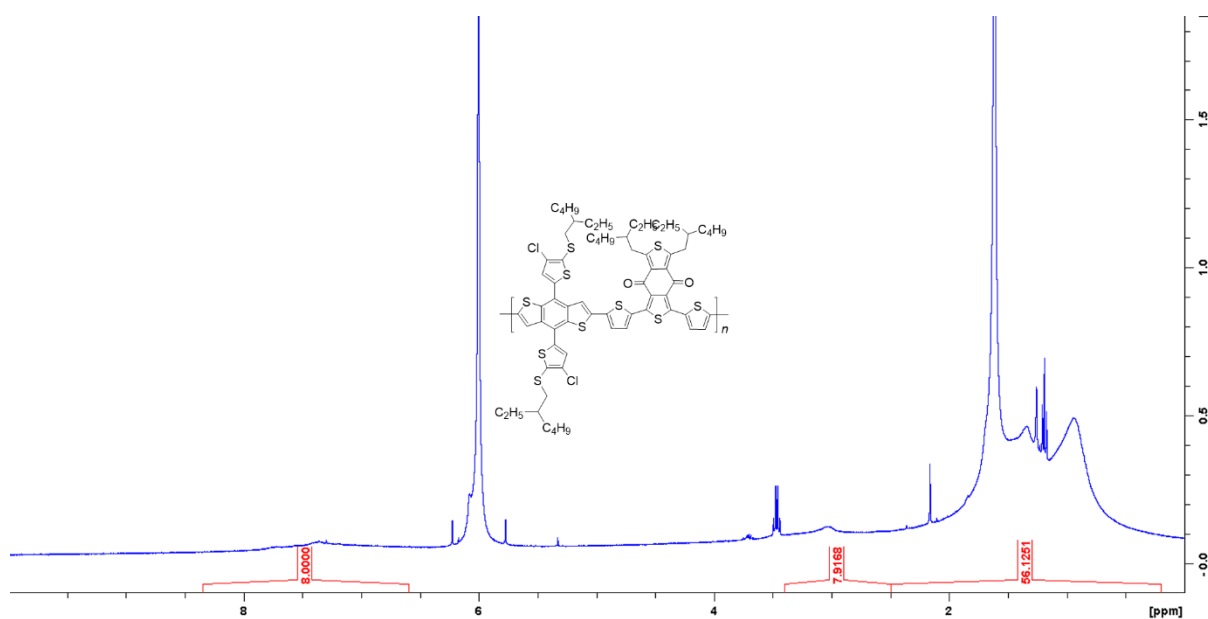


Figure S15. <sup>13</sup>C-NMR spectrum of compound 5



**Figure S16.** <sup>1</sup>H-NMR spectrum of PBDB-TSCl polymer in C<sub>2</sub>D<sub>2</sub>Cl<sub>4</sub>

## Reference

- (1) Zhang, M.; Gue, X.; Ma, W.; Ade H.; Hou, J. A Large-Bandgap Conjugated Polymer for Versatile Photovoltaic Applications with High Performance. *Adv. Mater.* **2015**, *27*, 4655.
- (2) Zhang, S.; Qin, Y.; Zhu J.; Hou, J. Over 14% Efficiency in Polymer Solar Cells Enabled by a Chlorinated Polymer Donor. *Adv. Mater.* **2018**, *30*, 1800868.
- (3) Hong, S.; Kang, H.; Kim, G.; Lee, S.; Kim, S.; Lee, J.-H.; Lee, J.; Yi, M.; Kim, J.; Back, H.; Kim, J.-R.; Lee, K. A series connection architecture for large-area organic photovoltaic modules with a 7.5% module efficiency. *Nat. Commun.* **2016**, *7*, 10279.
- (4) Malliaras, G. G.; Salem, J. R.; Brock, P. J.; Scott, C. Electrical characteristics and efficiency of single-layer organic light-emitting diodes. *Phys. Rev. B* **1998**, *58*, R13411.
- (5) Goh, C.; Kline, R. J.; McGehee, M. D.; Kadnikova, E. N.; Frechet, J. M. J. Molecular-weight-dependent mobilities in regioregular poly(3-hexyl-thiophene) diodes. *Appl. Phys.*

*Lett.* **2005**, 86, 122110.